Quantification of Local Hydration at the Surface of Biomolecules Using Dual-Fluorescence Labels

ARTICLE *in* THE JOURNAL OF PHYSICAL CHEMISTRY A · MARCH 2012

Impact Factor: 2.69 · DOI: 10.1021/jp2101732 · Source: PubMed

THE JOURNAL OF PHYSICAL CHEMISTRY A

Article

pubs.acs.org/JPCA

Quantification of Local Hydration at the Surface of Biomolecules Using Dual-Fluorescence Labels

Vasyl G. Pivovarenko,*[,†,‡] Oleksandr M. Zamotaiev,[†] Volodymyr V. Shvadchak,[‡] Viktoriia Y. Postupalenko,[‡] Andrey S. Klymchenko,[‡] and Yves Mély[‡]

[†]Organic Chemistry Chair, Chemistry Faculty, Taras Shevchenko National University of Kyiv, 01601 Kyiv, Ukraine

[‡]Laboratoire de Biophotonique et Pharmacologie, UMR 7213 du CNRS, Université de Strasbourg, Faculté de Pharmacie, 74 route du Rhin, 67401 Illkirch, France

Supporting Information

ABSTRACT: By using four labels of the 3-hydroxyflavone family displaying selective sensitivity to hydrogen bond (HB) donors and poor response to other polar molecules, we developed an approach for measuring local water concentration $[H_2O]_L$ (or partial volume of water: $W_A = [H_2O]_L/55.6$) in the label surrounding both in solvent mixtures and in biomolecules by the intensity ratio of two emissive forms of the label, N^*/T^*. Using a series of binary water/solvent mixtures with limited preferential solvation effects, a linear dependence of $\log(N^*/T^*)$ on the local concentration of HB donor was obtained and then used as a calibration curve for estimating the W_A values in the surroundings of the probes conjugated to biomolecules. By this approach, we estimated the hydration of the labels in different peptides and their complexes with DNAs. We found that W_A values for the label at the peptide N-terminus are lower (0.63−0.91) than for free labels and depend strongly on the nature of the N-terminal amino acid. When complexed with different DNAs, the estimated hydration of the labels conjugated to the labeled peptides was much lower (W_A = 0−0.47) and depended on the DNA nature and linker-label structure. Thus, the elaborated method allows a site-specific evaluation of hydration at the surface of a biomolecule through the determination of the partial volume of water. We believe the developed procedure can be successfully applied for monitoring hydration at the surface of any biomolecule or nanostructure.

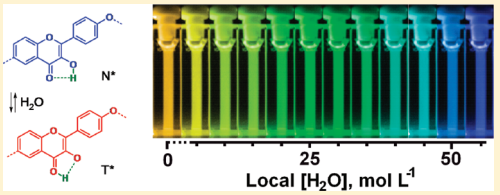

INTRODUCTION

Water plays a large variety of roles in biological systems at different levels of complexity, from molecules and cell organelles to tissues.[1−4] As an essential functional component, water is always present in the interior of biomolecules. At the surface of biomolecules, such as proteins, nucleic acids, or lipid aggregates, the properties of water change dramatically depending on the chemical nature of the solvated segment and the water−segment distance.[1,5−8]

Until now, main attention was paid to the study of water located in the interior of biomolecules or at the surface of lipid and protein assemblies.[1−4,9−16] IR, near-IR vibrational spectroscopy,[12,13] terahertz spectroscopy,[5] neutron and X-ray scattering,[12] and magnetic resonance methods[10] are usually applied in these studies.[1,17−25] Electron spin resonance (ESR) of molecular aggregates incorporating spin-labeled lipid units was shown to be a powerful approach[24] for determining hydrogen-bonding with water at various locations in the fluid membrane.[17,24,26]

Fluorescence probing is also an important tool for characterizing the hydration of biopolymers and its changes during biological processes.[1,4,27−32] For instance, polarity-sensitive fluorescent probes efficiently report on the hydration of supramolecular assemblies,[4] while Prodan,[28−31] phthalimide or naphthalimide,[28,32−35] and Nile Red[28,36] derivatives are common tools for lipid membranes[30,31,36] and for monitoring peptide binding to nonpolar proteins.[28,32−36] However, applications of polarity sensors to hydration studies are limited to relatively nonpolar systems, where the response of these dyes to polarity is high. In polar media, their fluorescence is quenched at higher water concentration[34] or is poorly sensitive to water.

3-Hydroxychromones (3HC) and, particularly, 3-hydroxyflavones (3HFs) appear as very attractive tools for studying hydration of biomolecules and their complexes.[37−56] These probes undergo excited-state proton transfer (ESIPT) that results in two emission bands. The rate of the ESIPT reaction and therefore the relative intensity of the normal (N^*) and tautomeric (T^*) bands depends on the properties of their molecular surroundings. The sensitivity of 3HF dyes to protic solvents is mainly due to H-bond formation with the groups involved in the ESIPT reaction (3-OH and 4-keto groups).[57,58] Because of their extreme sensitivity to traces of water in organic medium,[38,39] 4′-amino derivatives of 3HFs were used for the evaluation of hydration of lipid membranes at different locations.[40,41,45−47,49,50] Recently, improved 3HC derivatives were synthesized and successfully applied for site-selectively investigating the physicochemical properties, and notably, the

Received: October 23, 2011
Revised: February 15, 2012
Published: March 6, 2012

polarity and hydration of lipid membranes, proteins, and nucleic acids.[43,48,50−55]

However, the quantification of the local water content $[H_2O]_L$ at a given location of a biomolecular system using fluorescent probes has been never addressed so far. For most hydration-sensitive probes, quantification of $[H_2O]_L$ is a complex problem as a result of the overlapping responses of the probes to water and various parameters of their environment (e.g., polarity) as well as to their interactions with surrounding molecules and ions. Thus, to quantify the local water content, the chemical structure of the fluorescent probes needs to be optimized so that H-bonding dominates over the effects of dipole−dipole and ionic interactions and over the other physicochemical properties of the surroundings. Recently, a step toward this aim was achieved by the design of four 3HF probes that show strong sensitivity to hydration changes and negligible response to polarity and basicity.[54]

In this work, we propose a method for measuring the local water content at the labeling site of peptides, based on the ratiometric response of 3HF fluorophores and the application of this method for comparing the hydration levels of peptides in their free state and in peptide−DNA complexes.

MATERIALS AND METHODS

Reagents and Solvents. All the reagents were purchased from Sigma-Aldrich. Solvents for synthesis were of reagent quality and were appropriately dried if necessary. For absorption and fluorescence studies, the solvents were of spectroscopic grade. Calf thymus DNA (CT-DNA), cTAR, and single-stranded DNA poly(dA) and poly(dT) were from Sigma.

Synthesis of FC, F6A, and F4O compounds were published elsewhere.[54,55] Lipophilicity coefficients log *P* of the applied probes were calculated by ACD/Laboratories software. To more accurately measure the hydration parameters of the peptides labeled by the F6C probe, the amide derivative of free probe (F6Ca) was synthesized (see Supporting Information) and characterized spectroscopically.

3-Hydroxy-2-(4-methoxyphenyl)-4-oxo-4*H*-6-chromenecarboxamide (F6Ca). ^{1}H-NMR (400 MHz, DMSO-d_6). Abbreviations: s, singlet; d, doublet; m, multiplet; brs, broad singlet. δ, ppm: 3.87 (s, 3H, O**CH**$_3$), 7.05 (d, 2H, J = 8.8 Hz, Ar**H**), 7.31 (brs, 1H, N**H**), 7.70 (d, 1H, J = 8.8 Hz, Ar**H**), 8.20 (m, 4H, Ar**H**), 8.67 (brs, 1H, N**H**), 9.35 (brs, 1H, **OH**). Calc for $C_{17}H_{14}NO_5^+$ m/z ($M + H^+$): 312.087. Found: 312.087.

Peptide Synthesis. All peptides were synthesized by solid phase peptide synthesis on a 433A synthesizer (ABI, Foster City, CA) as published elsewhere.[54,60]

Sample Preparation. To the solution of probe (~2×10^{-6} mol L^{-1}) in a chosen organic solvent, aqueous solutions with equal probe concentration were added in the quantities needed for obtaining final water concentrations of 4, 8, 11, 14, 18, 22, 25, 27.5, and 30 mol L^{-1}. A second series was obtained by mixing the probe solution in organic solvent with its aqueous solution in the quantities needed for obtaining final water concentrations of 53, 51, 49, 47, 45, 42, 37, 33, 30, and 27.5 mol L^{-1}. For probes F6Ca and FC, a more close-packed set of water concentrations was applied. Fluorescence spectra of the obtained solutions including those in neat water and neat solvent were measured at 25 °C, immediately after preparation, using an excitation wavelength corresponding to the maximum of the absorption band.

Instrumentation. Proton NMR spectra were recorded on a 300 MHz Bruker spectrometer, and mass spectra were recorded on a Mariner System 5155 mass spectrometer using the electrospray ionization (ESI) method. All column chromatography experiments were performed on silica gel (Merck, Kieselgel 60H, Art 7736). Absorption and fluorescence spectra were recorded on a Cary 400 spectrophotometer (Varian) and FluoroMax 3.0 spectrofluorimeter (Jobin Yvon, Horiba), respectively. For fluorescence studies, the dyes were used at 0.5 to 1 × 10^{-6} mol L^{-1} concentrations. Excitation wavelength was on the absorption maximum for each label. Fluorescence quantum yields were determined using quinine sulfate in 0.5 mol L^{-1} sulfuric acid, as a reference (quantum yield, φ = 0.57).[59] For the experiments in water, 10^{-2} mol L^{-1} phosphate buffer containing 3 × 10^{-2} mol L^{-1} NaCl (pH 7.0) was used systematically. All spectroscopic data for labeled peptides and their complexes with DNA are from the literature.[54,55,60]

Deconvolution of Spectra. Deconvolution of the fluorescence spectra into *N** and *T** bands was performed using the Siano software kindly provided by Professor A. O. Doroshenko (Kharkiv, Ukraine), as previously described.[61] The program is based on an iterative nonlinear least-squares method, where the individual emission bands were approximated by a log-normal function accounting for several parameters: maximal amplitude, I_{max}, spectral maximum position, ν_{max}, and position of half-maximum amplitudes, ν_1 and ν_2, for the blue and red parts of the band, respectively. These parameters determine the shape parameters of the log-normal function, namely, the full width at the half-maximum, fwhm = $\nu_1 - \nu_2$, and the band asymmetry, $P = (\nu_1 - \nu_{max})/(\nu_{max} - \nu_2)$. All parameters were allowed to vary in the iteration process, which allowed a good correlation of the separated bands with the initial spectrum (number of repetitions: ≥6; $R \geq 0.998$ for the experiments with peptides and DNAs, and $R \geq 0.9998$ for solvent mixtures. See Figures 1C and S2−S5 in the Supporting Information). In the case of spectra from neat water, five separately obtained spectra were subjected to the deconvolution procedure: $R \geq 0.9$. In this case, the fwhm parameter of the *T** band was taken from the data of appropriate binary solvent mixtures and then fixed upon deconvolution. The resulting integral fluorescence intensities of the separated *N** and *T** bands were used for calculation of the *N**/*T** ratio.

RESULTS AND DISCUSSION

Selected Probes and Mechanism of Water Sensing. In contrast to numerous dialkylamino-derivatives of 3HFs[39−42,45−47,49,50] that show strong sensitivity to both nonspecific dipolar and specific H-bonding interactions, the four 3HF derivatives recently synthesized by us (Scheme 1) are mainly sensitive to H-bonding interactions.[54,55] Indeed, for the four probes, it has been shown that H-bonding with the solvent, but not the solvent polarity, governs their *N**/*T** ratio and the position of their *T** band.[54,55] Moreover, their fluorescence properties were also found to be poorly dependent on the pH[54,56] and ionic strength (Figure 1A). Thus, the four 3HF derivatives appear as suitable candidates for measuring local water concentrations in biomolecules. Since the four compounds are characterized by different linker length and position, it will be possible to select the most appropriate ones for labeling a given biomolecule and investigate its interaction with target molecules.

In biological media, water molecules are the main H-bond (HB) donors. Assuming that the mechanism of the 3HF response to water molecules is the same when the probe is

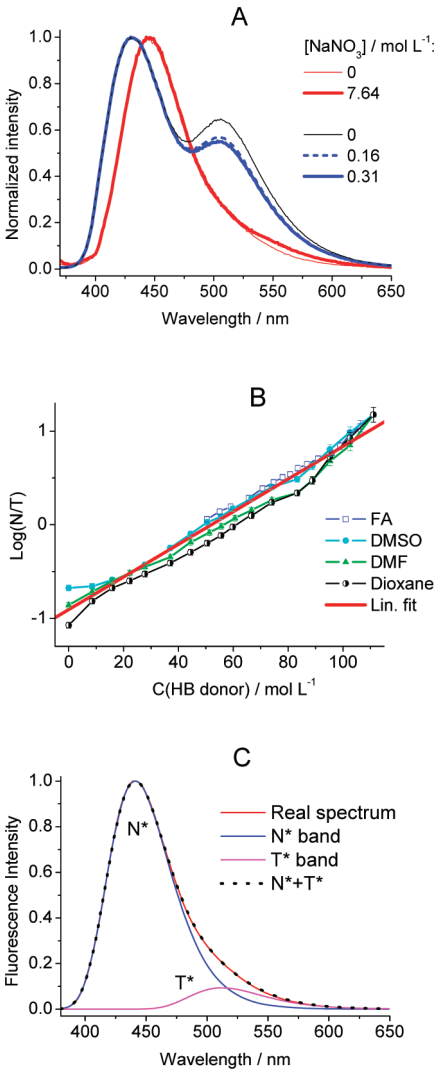

Figure 1. Dependence of the emission of 3HF probes on ionic strength and the molar concentration of hydrogen bond donor. (A) Influence of ionic strength on the emission of F6Ca (red) and FC (blue) probes in 10 mM phosphate buffer, pH 7.0. Excitation wavelength was fixed at the absorption maximum in each case. (B) Dependence of $\log(N^*/T^*)$ versus molar concentration of hydrogen bond donor in water–solvent mixtures for F6Ca probe. Since water and formamide possess two HB donor groups, we use $C_{HBdonor} = 2C_{solvent}$ for these solvents. (C) Example of deconvolution of the spectrum of F6Ca probe in water in two bands.

bound to biomolecules than when it is free, the probe response will result from the interaction of the 3HF atoms involved in ESIPT with water molecules. The mechanism is depicted in Scheme 2 (partially taken from ref 57). Through H-bonding with the 4-carbonyl group of 3HF dyes, water molecules weaken the intramolecular hydrogen bond and thus slow down or even block the intramolecular proton transfer.[57,58] Therefore, when bound to a biomolecule, an increasing exposure of the probe to water molecules within the solvation shell should increase the number of H-bonds, resulting in an increase of the N^*/T^* ratio and a blue shift of the T^* form.[54,58] Interference of HB-donating groups on the biomolecule (NH, OH, etc.) in the measurements of water concentration is unlikely, especially at the biomolecule surface, due to their relatively small concentration in respect to water.

Scheme 1. ESIPT Reaction in the 3HF Dyes and Structure of the Studied Labels and Labeled Peptides

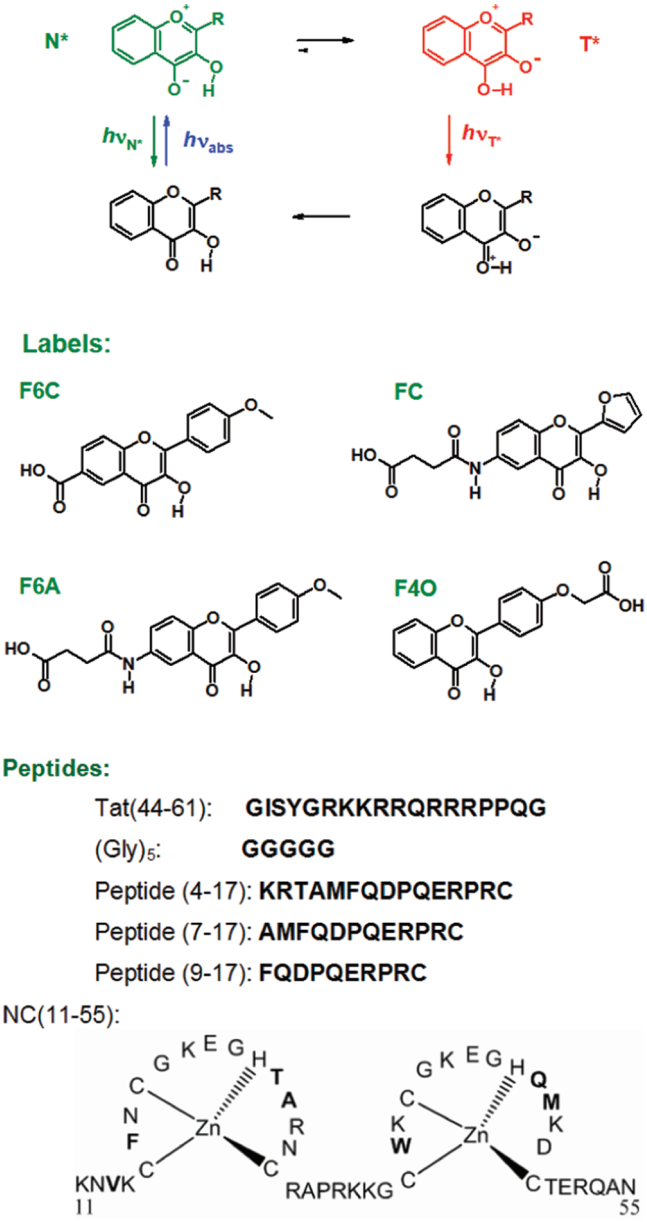

Calibration of Probe Response to H-Bond Donors. To calibrate the probe response to local water concentration $[H_2O]_L$, we measured the energy-related spectroscopic parameters of all labels in binary solvent–water mixtures and neat solvents. To ensure a more precise calibration for the peptide-bound label F6C, we transformed the F6C probe into its amide F6Ca, which is chemically closer to the form of the probe attached to the peptides. For other 3HCs, this modification should not play any role as their carboxylic group is electronically isolated from the fluorophore.

The $\log(N^*/T^*)$ parameter of the probe fluorescence was found appropriate for quantification of water concentration in the probe surroundings. In Figure 1B, as an example, the $\log(N^*/T^*)$ parameter of F6Ca is shown as a function of the total molar concentration of HB donors in the mixture. The log-scale was used in order to convert the N^*/T^* ratio into a parameter linearly correlating with the solvent concentration.[39] Linear correlation in such coordinates displays that the N^*/T^*

dx.doi.org/10.1021/jp2101732 | J. Phys. Chem. A 2012, 116, 3103–3109

Scheme 2. Chemical Mechanism of Water Sensing by the 3HF Probes[a]

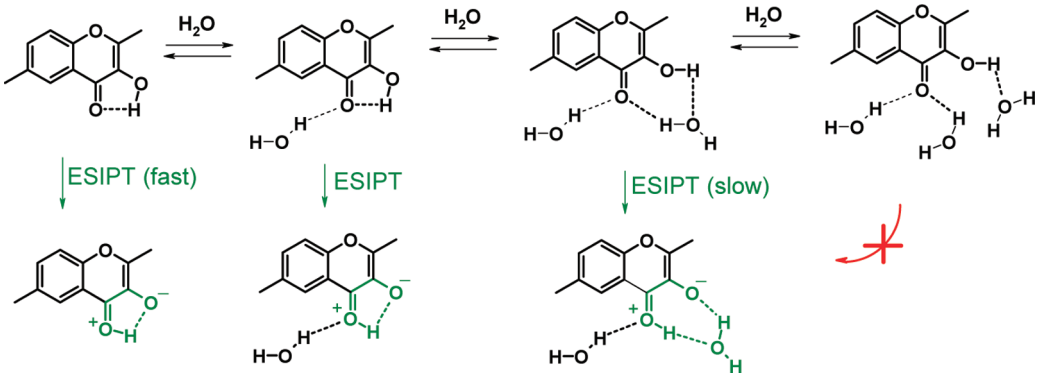

[a]Increasing levels of exposure to water of the 3HF probe bound to a biomolecule is thought to result in an increase in the number of H-bonds with the water molecules within the solvation shell.

parameter, the ratio of the two emissive populations of the probe, is driven by the chemical potential of water in the applied systems. The $\log(N^*/T^*)$ parameter according to the Boltzmann equation is proportional to the energy difference between the states, when they are in equilibrium. This is the case for 3HF probes in organic solvents[62] and should be also true for water solvates, for which relaxation times are much shorter.[1,4,7]

A linear correlation was observed in mixtures of water with formamide, dioxane, DMF, and DMSO, suggesting that the chemical potential of water (or water activity,[63] more roughly, water concentration) drives the N^*/T^* ratio of the emitting tautomers. The linearity also shows that the local concentration of water $[H_2O]_L$ in the probe solvation shell corresponds to the total concentration of water $[H_2O]_T$ in the mixtures.

In contrast, for some other solvent mixtures, the water concentration in the probe solvation shell differs from that in bulk solution since the concentration of each species in the probe solvation shell depends on its energy of interaction with the probe molecule. As a result, the energy-related parameters of probe fluorescence show nonlinear dependence upon the total concentration of the active component in the mixture.[64] Such phenomenon is known as the preferential solvation effect.[64,65] Such preferential solvation of the probe by water or by the organic solvent result in substantial upward and downward deviations from the linearity in the dependence of $\log(N^*/T^*)$ as a function of the total water concentration (Supporting Information, Figure S4). For instance, the strong HB-donor water molecules dominate over acetonitrile in the solvation shell (Supporting Information, Figure S4 upward deviations), while lipophilic 2-propanol and, especially, tetrahydrofurane dominate over water (Supporting Information, Figure S4, downward deviations). The level and sign of the observed deviations are in line with the chemical properties of solvent (e.g., its lipophilicity and HB-donating and HB-accepting coefficients, Table S2, Supporting Information). Upward deviations were also observed for binary mixtures of methanol, methylformamide (Figure S4, Supporting Information), and trifluoroethanol (not shown), whose aggregates with water possess increased HB-donating ability.

On the basis of the four water–solvent mixtures providing a linear dependence of $\log(N^*/T^*)$, a linear calibration curve was determined: $\log(N^*/T^*) = 0.0164[H_2O]_L - 0.695$ ($R = 0.978$) (Figure 1B, red line). At high water concentrations, a preferential solvation effect gives small deviations from the data point in neat water. Accordingly, these data points were removed from the calibration curve and substituted by the data point in neat water.

Next, using the same approach, we determined the calibration curves for the three other probes and found out that the calibration curves for F6A, F4O, and F6Ca were similar, while that for FC exhibited a nearly 2-fold smaller slope (Figure 2), indicating that FC is less sensitive to hydration.

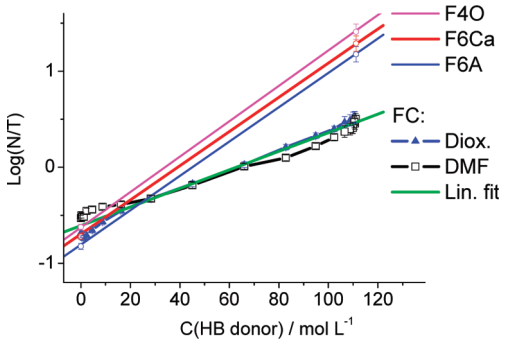

Figure 2. Dependence of $\log(N^*/T^*)$ on the concentration of hydrogen bond donor for the four 3HC derivatives. Fitted lines: F4O, $\log(N^*/T^*) = 0.0184[H_2O]_L - 0.627$; F6Ca, $\log(N^*/T^*) = 0.0177[H_2O]_L - 0.706$; F6A, $\log(N^*/T^*) = 0.0179[H_2O]_L - 0.805$; FC, $\log(N^*/T^*) = 0.0100[H_2O]_L - 0.607$.

Comparing the calibration curves with the titration curves in Figure 1, it is quite obvious that the error in the estimation of hydration will be much higher at low hydration levels, where the solvent effects other than hydration play an important role. The data points for polar (DMF and DMSO) and low polar solvents (e.g., dioxane) are close at water concentrations higher than 5 mol L^{-1}, which suggests a 5 mol L^{-1} limit for the precise estimation of water concentrations. Below this limit, non-specific dipolar interactions (i.e., solvent polarity) start interfering with the analysis. This concentration range is likely appropriate for proteins and oligonucleotides as well as their complexes, but not for lipid membrane sites, where the water concentration is usually below this range.[11,12]

From the mechanism presented in Scheme 2, it is obvious that the fluorescent probe senses only water in its close proximity, which allows quantifying the water concentration in the probe solvation shell. Since the probe response was related to the total concentration of water in our calibration procedure,

dx.doi.org/10.1021/jp2101732 | J. Phys. Chem. A 2012, 116, 3103–3109

we obtain in fact an average value of the local water concentration $[H_2O]_L$ in the probe solvation shell, that depends on the average location, orientation dynamics, and fluorescence lifetime of all peptide-conjugated probes in solution.

Hydration Measurements in Labeled Peptides and Their Complexes with Oligonucleotides. We already reported[54] that the Tat(44−61) peptide, corresponding to the basic domain of the HIV-1 protein,[66] labeled by the applied probes, showed a decrease of their N^*/T^* ratio (Table 1), when interacting with DNA sequences of various lengths and strandedness. The decrease in N^*/T^* ratio appears as a result of possible stacking of the probes with nucleic bases, which leads to a decrease of the probe hydration. Now, we show the possibility to quantify the hydration level at the location of the probe. As an application, we calculated the hydration of the FC probe bound to the N-terminus of a pentaglycine peptide,[55] the zinc finger domain of the HIV-1 nucleocapsid protein (NC),[55,67] and several peptide sequences (4−17, 7−17, and 9−17),[60] which contain the binding site recognized by an antibody fragment, $scFv1F4_{Q34S}$.

Table 1. Intensity Ratios of Fluorescence Bands and Hydration Parameters for the Applied Probes in Their Peptide Conjugates and Peptide−DNA Complexes[a]

	N^*/T^* ratio	$[H_2O]_L$	W_A
F6Ca (1.4)[b]	18	55.5	1.0
F6C−Tat	4.64	38.3	0.69
F6C−Tat + poly dT	0.44	9.4	0.17
F6C−Tat + CT-DNA	0.32	5.75	0.10
FC (−0.33)[b]	3.2	55.5	1.0
FC−Tat	1.8	43.0	0.77
FC−Tat + poly dT	0.65	20.9	0.38
FC−Tat + poly dA	0.82	26.0	0.47
FC−Tat + CT-DNA	0.51	15.6	0.28
FC−NC	1.7	41.8	0.75
FC−$(Gly)_5$	2.25	48.0	0.86
FC(4−17)	1.7	42.3	0.76
FC(7−17)	2.5	50.3	0.91
FC(9−17)	1.3	36.5	0.66
F6A (0.46)[b]	15	55. 5	1.0
F6A−Tat	6.5	43.0	0.77
F6A−Tat + poly dT	0.53	15.9	0.29
F6A−Tat + CT-DNA	0.32	10.0	0.18
F4O (0.98)[b]	25	55.5	1.0
F4O−Tat	4.7	35.3	0.63
F4O−Tat + poly dT	0.44	7.4	0.13
F4O−Tat + poly dA	0.53	9.6	0.17
F4O−Tat + cTAR	0.29	~2.5	~0.05
F4O−Tat + CT-DNA	0.19	~0	~0

[a] $[H_2O]_L$ is the local water concentration (mol L^{-1}) calculated from the calibration curves in Figure 2. W_A is the local water access coefficient. [b] Logarithm of the distribution coefficient of the amide derivatives of the probes in 1-octanol−water mixture (log P).

For biomolecules and their complexes, it is more convenient to express the level of hydration through the water access coefficient W_A of the probe:

$$W_A = [H_2O]_L/[H_2O] = [H_2O]_L/55.56$$

where $[H_2O]$ is the molar concentration of neat water.

W_A shows the fraction of space in the surrounding of the probe proton-transfer system, occupied by water molecules. W_A is also called the partial volume of water and is frequently used for characterization of hydration.[11,12]

Using this approach, we calculated the hydration level for several peptides in 10^{-2} mol L^{-1} phosphate buffer containing 3 × 10^{-2} mol L^{-1} NaCl (pH 7.0).[54,60] We found that the W_A values of the probes in their conjugates with the N-terminus of the Tat peptides was 20−40% lower than the W_A value of the probe alone (Table 1). The observed W_A values were the lowest (Figure 3A) for the F6C and F4O probes, which present the highest lipophilicity coefficients (log P = 1.4 and 0.98, respectively, Table 1). These rather low W_A values are likely the result of the stronger interaction of these dyes with the more hydrophobic components of the peptide, which reduces the

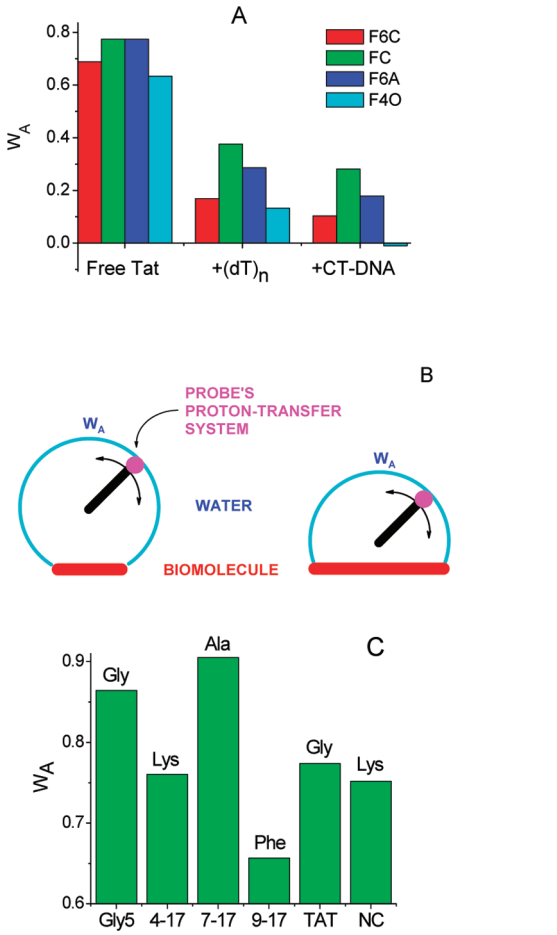

Figure 3. Water access W_A coefficients for peptides labeled by the 3HF probes. (A) The water access for the Tat(44−61) peptide labeled by either the F6C, FC, F6A, and F4O probe was determined in the absence and in the presence of poly dT or CT-DNA. (B) Representation of the decrease of local water access W_A caused by the probe lipophilicity. The rotational motion of the label is represented by an arc, whose length reflects the measured W_A value. The sphere delineated by the arc represents the accessible volume for W_A measurements. A more lipophilic label (right) is thought to interact more strongly than a less lipophilic one (left) with the biomolecule and thus lead to a smaller W_A value. (C) Dependence of the water access on the nature of the peptide and N-terminal amino acid. The W_A coefficients are given for FC-labeled $(Gly)_5$, peptide (4−17), peptide (7−17), peptide (9−17), Tat(44−61), and NC peptide. The nature of the N-terminal amino acid is indicated over the bars.

dx.doi.org/10.1021/jp2101732 | J. Phys. Chem. A 2012, 116, 3103−3109

volume of accessible water (Figure 3B). Moreover, as these probes are connected to the peptide through a shorter linker, their screening from bulk water is likely more efficient.

On the next step, we studied the effect of the peptide sequence on the probe hydration. Remarkably, the W_A values vary significantly with the N-terminally labeled peptide sequence (Figure 3C). Thus, in $(Gly)_5$ and peptide (7−17), the W_A value is the highest, while for peptide (9−17), it is the lowest. However, peptide 4−17, Tat(44−61), and NC show intermediate values of hydration. Comparison of the sequences suggests that the closest amino acid residues influence the label hydration. For instance, the low W_A value for peptide (9−17) can be correlated with the presence of the highly hydrophobic and rather bulky N-terminal Phe amino acid, which likely screens efficiently the label from bulk water, while high W_A values are observed when the N-terminal residue is Gly.

Interaction of the labeled Tat(44−61) peptides with poly dT and poly dA DNA was found to dramatically decrease the hydration level of the probes (Table 1), likely as a consequence of the stacking of the probes with the bases of these single-stranded (*ss*) nucleic acids. The W_A values in poly dT were somewhat lower than in poly dA, indicating that interaction with dT bases provided better screening from the bulk water. A further decrease in the hydration of the probes was observed when the Tat peptides were bound to the double-stranded (ds) CT-DNA (Figure 3A), likely as a result of the intercalation of the probe between the DNA base pairs.[54] The data for F6C, F6A, and FC show a correlation between the W_A and log *P* values, as the probes demonstrate a decrease in the W_A values with the increase of their lipophilicity coefficients. Thus, the intercalation between the bases is more efficient for less polar labels, which results in decreased water access W_A values (Figure 3B).

Interestingly, the W_A value for the F4O probe in the peptide−DNA complexes is much lower than for the other probes, suggesting that this probe has almost no access to water in the peptide−dsDNA complex. The peculiar behavior of this probe in respect to the three others can be rationalized by considering the possible intercalation of the various probes in the peptide−DNA complexes. We could speculate that the structure of the F4O dye favors the deep insertion of the atoms participating to ESIPT within the base pairs, allowing efficient screening from the water (Figure 4). In contrast, for the three other probes, the insertion of the ESIPT atoms within the base pairs is less deep, so that water accessibility is still possible.

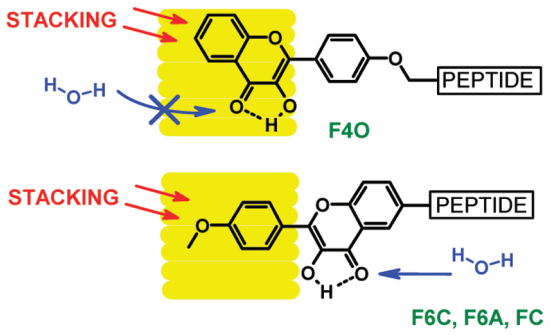

Figure 4. Directions of hydrogen bonding and stacking interactions for the various probes. The interior of DNA base pairs is marked by yellow.

CONCLUSIONS

In this study, we developed a new approach for the estimation of local water concentration using recently developed dual-fluorescence 3HF labels displaying selective sensitivity to HB donors. For these probes in binary solvent mixtures showing no preferential solvation effect, a linear dependence was obtained for $\log(N^*/T^*)$, the logarithm of the emission intensity ratio of two bands versus the local concentration of HB donor. Because of the poor sensitivity of the probes to dipolar molecules, pH, and ionic strength of the medium, the obtained calibration curve allowed us to quantitatively determine the hydration of the label, expressed as the partial volume of water in the label surroundings ($W_A = [H_2O]_L/55.6$). Using this approach, we determine the hydration level of the probes for different N-terminus-labeled peptides and their complexes with DNAs. We found that the hydration level of the labels in peptides was 10−40% lower than for the labels alone. Further comparison of the free labeled peptides shows that the lipophilicity and size of the N-terminal amino acid plays a key role on the label hydration. In complexes of Tat-peptides with ssDNA, the estimated hydration was much smaller, dependent on the label and the DNA bases. Moreover, with dsDNA, the hydration of the label was even lower indicating an efficient screening from water, likely through dye intercalation. We found that the measured value of hydration is dependent on the lipophilicity of the applied label and on the length and position of its connection to the linker since these features govern in part the location and dynamics of the label in the analyzed object. Quantitative analysis of hydration allowed us to further find out that the F4O label showed the lowest level of hydration (~0) in the complex of the Tat-peptide with dsDNA, as a consequence of its deeper insertion between the base pairs. Thus, we found that the water content in the label surrounding at the N-terminus of the peptide depends largely on the peptide nature and can reach almost zero values in complexes with dsDNA, where the label is efficiently screened from water. We believe that the developed procedure can be successfully applied for monitoring hydration of any biomolecule or nanostructure.

ASSOCIATED CONTENT

Supporting Information

Synthesis of F6Ca probe. Spectroscopic properties of F6C, F6Ca, F6A, F4O, and FC probes in different solvents. Dependence of $\log(N^*/T^*)$ versus molar concentration of hydrogen bond donor in water−solvent mixtures. Fluorescence spectra of labeled peptides alone and in the presence of DNAs. This material is available free of charge via the Internet at http://pubs.acs.org.

AUTHOR INFORMATION

Notes

The authors declare no competing financial interest.

ACKNOWLEDGMENTS

ARCUS program is acknowledged for financial support. V.G.P. is thankful to Université de Strasbourg for support of a one month stay.

REFERENCES

(1) Zhong, D.; Pal, S. K.; Zewail, A. H. *Chem. Phys. Lett.* **2011**, *503*, 1.
(2) Ball, P. *Chem. Rev.* **2008**, *108*, 74.
(3) Chaplin, M. *Nat. Rev. Mol. Cell. Biol.* **2006**, *7*, 861.

(4) Pal, S. K.; Zewail, A. H. *Chem. Rev.* **2004**, *104*, 2099.
(5) Fayer, M. D. *Acc. Chem. Res.* **2012**, *45*, 3.
(6) Shultz, M. J.; Vu, T. H.; Meyer, B.; Bisson, P. *Acc. Chem. Res.* **2012**, *45*, 15.
(7) Zhang, L.; Yang, Y.; Kao, Y.-T.; Wang, L.; Zhong, D. *J. Am. Chem. Soc.* **2009**, *131*, 10677.
(8) Ebbinghaus, S.; Kim, S. J.; Heyden, Y. X.; Heugen, U.; Gruebele, M.; Leitner, D. M.; Havenith, M. *Proc. Natl. Acad. Sci. U.S.A.* **2007**, *104*, 20749.
(9) Chalikian, T. V.; Macgregor, R. B. *Phys. Life Rev.* **2007**, *4*, 91.
(10) Gawrisch, K.; Gaede, H. C.; Mihailescu, M.; White, S. H. *Eur. Biophys. J.* **2007**, *36*, 281.
(11) Lomidze, A. L.; Pogozheva, I. D.; Mosberg, H. I. *J. Chem. Inf. Model.* **2011**, *51*, 930.
(12) Kucerka, N.; Nagle, J. F.; Sachs, J. N.; Feller, S. E.; Pencer, J.; Jackson, A.; Katsaras, J. *Biophys. J.* **2008**, *95*, 2356.
(13) Marsh, D. *Biophys. J.* **2008**, *94*, 3996.
(14) Bagchi, B. *Chem. Rev.* **2005**, *105*, 3197.
(15) Khoshtariya, D. E.; Hansen, E.; Leecharoen, R.; Walker, G. C. *J. Mol. Liq.* **2003**, *105*, 13.
(16) Waegele, M. M.; Tucker, M. J.; Gai, F. *Chem. Phys. Lett.* **2009**, *478*, 249.
(17) Kurad, D.; Jeschke, G.; Marsh, D. *Biophys. J.* **2003**, *85*, 1025.
(18) Marsh, D. *Proc. Natl. Acad. Sci. U.S.A.* **2001**, *98*, 7777.
(19) Marsh, D. *Eur. Biophys. J.* **2002**, *31*, 559.
(20) Furo, I. *J. Mol. Liq.* **2005**, *117*, 117.
(21) Bryant, G.; Pope, J. M.; Wolfe, J. *Eur. Biophys. J.* **1992**, *21*, 223.
(22) Hawton, M. H.; Doane, J. W. *Biophys. J.* **1987**, *52*, 401.
(23) Volke, F.; Pampel, A. *Biophys. J.* **1995**, *68*, 1960.
(24) McCarney, E. R.; Armstrong, B. D.; Kausik, R.; Han, S. *Langmuir* **2008**, *24*, 10062.
(25) Xu, Z. C.; Ellena, J. F.; Cafiso, D. S. *Biophys. J.* **1986**, *49*, A508.
(26) Owenius, R.; Engstrom, M.; Lindgren, M.; Huber, M. *J. Phys. Chem. A* **2001**, *105*, 10967.
(27) Meulen, K. A. V.; Saecker, R. M.; Record, M. T. Jr. *J. Mol. Biol.* **2008**, *377*, 9.
(28) Loving, G. S.; Sainlos, M.; Imperiali, B. *Trends Biotechnol.* **2010**, *28*, 73.
(29) Kucherak, O. A.; Didier, P.; Mely, Y.; Klymchenko, A. S. *J. Phys. Chem. Lett.* **2010**, *1*, 616.
(30) Lee, J. C.-M.; Law, R. J.; Discher, D. E. *Langmuir* **2001**, *17*, 3592.
(31) Zhang, Y.-L.; Frangos, J. A.; Chachisvilis, M. *Biochem. Biophys. Res. Commun.* **2006**, *347*, 838.
(32) Loving, G.; Imperiali, B. *Bioconjugate Chem.* **2009**, *20*, 2133.
(33) Sainlos, M.; Imperiali, B. *Nat. Protoc.* **2007**, *2*, 3210.
(34) Loving, G.; Imperiali, B. *J. Am. Chem. Soc.* **2008**, *130*, 13630.
(35) Venkatraman, P.; Nguyen, T. T.; Sainlos, M.; Bilsel, O.; Chitta, S.; Imperiali, B.; Stern, L. J. *Nat. Chem. Biol.* **2007**, *3*, 222.
(36) Kucherak, O. A.; Oncul, S.; Darwich, Z.; Yushchenko, D. A.; Arntz, Y.; Didier, P.; Mely, Y.; Klymchenko, A. S. *J. Am. Chem. Soc.* **2010**, *132*, 4907.
(37) McMorrow, D.; Kasha, M. *J. Phys. Chem.* **1984**, *88*, 2235.
(38) Liu, W.; Wang, Y.; Jin, W.; Shen, G.; Yu, R. *Anal. Chim. Acta* **1999**, *383*, 299.
(39) Klymchenko, A. S.; Demchenko, A. P. *Phys. Chem. Chem. Phys.* **2003**, *5*, 461.
(40) Klymchenko, A. S.; Duportail, G.; Demchenko, A. P.; Mély, Y. *Biophys. J.* **2004**, *86*, 2929.
(41) Shynkar, V. V.; Klymchenko, A. S.; Piémont, E.; Demchenko, A. P.; Mély, Y. *J. Phys. Chem. A* **2004**, *108*, 8151.
(42) Klymchenko, A. S.; Kenfack, C.; Duportail, G.; Mely, Y. *J. Chem. Sci.* **2007**, *119*, 83.
(43) Klymchenko, A. S.; Shvadchak, V. V.; Yushchenko, D. A.; Jain, N.; Mely, Y. *J. Phys. Chem. B* **2008**, *112*, 12050.
(44) Das, R.; Klymchenko, A. S.; Duportail, G.; Mély, Y. *Photochem. Photobiol. Sci.* **2009**, *8*, 1583.
(45) Klymchenko, A. S.; Mely, Y.; Demchenko, A. P.; Duportail, G. *Biochim. Biophys. Acta* **2004**, *1665*, 6.
(46) Oncul, S.; Klymchenko, A. S.; Kucherak, O. A.; Demchenko, A. P.; Martin, S.; Dontenwill, M.; Arntz, Y.; Didier, P.; Duportail, G.; Mély, Y. *Biochim. Biophys. Acta* **2010**, *1798*, 1436.
(47) M'Baye, G.; Mély, Y.; Duportail, G.; Klymchenko, A. S. *Biophys. J.* **2008**, *95*, 1217.
(48) van Hell, A. J.; Klymchenko, A.; Burgers, P. P.; Moret, E. E.; Jiskoot, W.; Hennink, W. E.; Crommelin, D. J.; Mastrobattista, E. *J. Phys. Chem. B* **2010**, *114*, 11046.
(49) Demchenko, A. P.; Mély, Y.; Duportail, G.; Klymchenko, A. S. *Biophys. J.* **2009**, *96*, 3461.
(50) Postupalenko, V. Y.; Shvadchak, V. V.; Duportail, G.; Pivovarenko, V. G.; Klymchenko, A. S.; Mély, Y. *Biochim. Biophys. Acta* **2011**, *1808*, 424.
(51) Yushchenko, D. A.; Fauerbach, J. A.; Thirunavukkuarasu, S.; Jares-Erijman, E. A.; Jovin, T. M. *J. Am. Chem. Soc.* **2010**, *132*, 7860.
(52) Enander, K.; Choulier, L.; Olsson, A. L.; Yushchenko, D. A.; Kanmert, D.; Klymchenko, A. S.; Demchenko, A. P.; Mely, Y.; Altschuh, D. *Bioconjugate Chem.* **2008**, *19*, 1864.
(53) Boudier, C.; Klymchenko, A. S.; Mely, Y.; Follenius-Wund, A. *Photochem. Photobiol. Sci.* **2009**, *8*, 814.
(54) Zamotaiev, O. M.; Postupalenko, V. Y.; Shvadchak, V. V.; Pivovarenko, V. G.; Klymchenko, A. S.; Mély, Y. *Bioconjugate Chem.* **2011**, *22*, 101.
(55) Shvadchak, V. V.; Klymchenko, A. S.; de Rocquigny, H.; Mely, Y. *Nucleic Acids Res.* **2009**, *37*, 885.
(56) Klymchenko, A. S.; Demchenko, A. P. *New J. Chem.* **2004**, *28*, 687.
(57) Strandjord, A. J. G.; Barbara, P. F. *J. Chem. Phys.* **1985**, *89*, 2355.
(58) Pivovarenko, V. G.; Wróblewska, A.; Błazejowski, J. *J. Mol. Struct.* **2004**, *708*, 175.
(59) Eastman, J. W. *Photochem. Photobiol.* **1967**, *6*, 55.
(60) Choulier, L.; Shvadchak, V. V.; Naidoo, A.; Klymchenko, A. S.; Mély, Y.; Altschuh, D. *Anal. Biochem.* **2010**, *401*, 188.
(61) Doroshenko, A. O.; Sychevskaya, L. B.; Grygorovych, A. V.; Pivovarenko, V. G. *J. Fluoresc.* **2002**, *12*, 455.
(62) Shynkar, V. V.; Mely, Y.; Duportail, G.; Piemont, E.; Klymchenko, A. S. *J. Phys. Chem. A* **2003**, *107*, 9522.
(63) Blandamer, M. J.; Engberts, J. B. F. N.; Gleeson, P. T.; Reis, J. C. R. *Chem. Soc. Rev.* **2005**, *34*, 440.
(64) Bakhshiev, N. G., Ed.; *Solvatochromism. Problems and Methods*; LGU: Leningrad, Russia, 1989.
(65) Salari, H.; Khodadadi-Moghaddam, M.; Harifi-Mood, A. R.; Gholami, M. R. *J. Phys. Chem. B* **2010**, *114*, 9586.
(66) Boudier, C.; Storchak, R.; Sharma, K. K.; Didier, P.; Follenius-Wund, A.; Muller, S.; Darlix, J. L.; Mély, Y. *J. Mol. Biol.* **2010**, *400*, 487.
(67) Darlix, J.-L.; Godet, J.; Ivanyi-Nagy, R.; Fossé, P.; Mauffret, O.; Mély, Y. *J. Mol. Biol.* **2011**, *410*, 565.